Accurate consideration of metal losses at waveguide junctions using admittance and impedance integral equation formulations

M. Taroncher,[1] J. Hueso,[1] S. Cogollos,[1] B. Gimeno,[2] V. E. Boria,[1] A. Vidal,[1]
H. Esteban,[1] and M. Guglielmi[3]

[1] At higher frequencies, metal loss effects in passive waveguide components become more pronounced and hazardous. In this paper, we propose two integral equation techniques, based on the generalized admittance and impedance matrices, for the accurate consideration of losses in the metal walls of waveguide junctions. Both techniques have been evaluated in terms of accuracy and numerical efficiency, and conclusions are drawn regarding the best properties of the admittance parameter formulation. Finally, combining such technique with a classical perturbative method for considering propagation losses, we have successfully predicted all loss effects in two real waveguide filters used for commercial applications.

1. Introduction

[2] The modeling of losses due to nonperfect conducting materials used in the fabrication of microwave components is a fundamental key for an accurate characterization of passive waveguide devices, such as filters, couplers, polarizers, orthomode transducers, diplexers and multiplexers [see *Matthaei et al.*, 1980; *Conciauro et al.*, 2000]. These components are key elements in most present and future wireless and/or space communication systems operating at higher frequencies (microwave and millimeter-wave bands), where the conventional approach of neglecting losses or considering them as a second-order effect, as followed by *Alvarez et al.* [1996], is no longer valid. In this high-demanding scenario, an accurate consideration of the metal loss effects within the present computer-aided design (CAD) tools of passive waveguide devices is required [see *Melloni and Gentilli*, 1995].

[3] The effect of losses in microwave waveguides and cavities has been under consideration in the technical literature during recent decades. A first approximation for the analysis of the metal losses only considers the attenuation of the power flow in the direction of propagation due to the finite conductivity of the waveguide metallic ones [see, e.g., *Balanis*, 1989; *Collin*, 1991]. In this perturbation method it is assumed that the electromagnetic fields for a given mode in the presence of finite conductivity walls are essentially the same as when the conductivity is infinite. As a consequence, the surface currents flowing on the guide walls can be directly calculated. Such approach permits to evaluate the losses in the walls from the known surface current density of the unperturbed mode, which directly leads to the calculation of the modal attenuation constant related to the propagation direction. Another very early contribution to the general properties of degenerated modes in lossy waveguides, which are treated by employing a variational method, can be found in work by *Gustincic* [1963]. However, all these perturbative approaches do not take into account the losses in the transversal metallic walls of the waveguide junctions, which can be important as proved by *Hueso et al.* [2004].

[4] Therefore, in order to increase the accuracy of modern CAD tools, the rigorous consideration of the losses due to the transversal metallic wall of a junction between two waveguides with different cross sections should be included. Up to now, very few techniques have

---
[1]Departamento de Comunicaciones, Universidad Politécnica de Valencia, Valencia, Spain.
[2]Instituto de Ciencia de los Materiales, Departamento de Física Aplicada, Universidad de Valencia, Valencia, Spain.
[3]European Space Research and Technology Centre, Noordwijk, Netherlands.

been developed in order to solve accurately junctions of waveguides with finite wall conductivity. For instance, an E field mode-matching method combined with the conservation of complex power technique was first proposed by *Wade and McPhie* [1990], whereas a pure mode-matching technique formulated in terms of electric and magnetic currents, and leading to the generalized scattering matrix (GSM) representation, can be found in work by *Trinchero et al.* [1997]. Both works show very interesting preliminary results, but information about numerical efficiency and convergence issues (i.e., the relative convergence phenomenon widely documented by *Leroy* [1983], *Itoh* [1989], and *Sorrentino et al.* [1991]) are missed. More recently, the longitudinal and transversal attenuation constants for a lossy waveguide (also including the presence of lossy dielectrics) have been evaluated by means of a nonperturbative technique by *Mattes and Mosig* [1999], but such an approach cannot presently deal with waveguide junctions.

[5] In this context, the objective of this work is to extend both admittance and impedance integral equation formulations, originally proposed by *Gerini et al.* [1998] for the lossless case, to the accurate consideration of metal losses in waveguide junctions. The basics of this theory for the generalized admittance matrix (GAM) formulation can be found in work by *Hueso et al.* [2004], where it was successfully applied to a few simple examples. In this paper, the theory extension for solving the same problem in terms of a generalized impedance matrix (GIM), as well as the efficient solution of both integral equation formulations, are detailed. Then a comparative study of GAM and GIM techniques in terms of numerical robustness and efficiency is presented, thus revealing the best performance of the admittance parameter formulation. Finally, combining the GAM technique with the classical perturbation method cited before [see *Balanis*, 1989; *Collin*, 1991], we have successfully predicted all loss effects in two real application prototypes: an inductive band-pass filter at 28 GHz for local multipoint distribution systems (LMDS) and a commercial filter composed of a band-pass and a low-pass section for a C band (6 GHz) communication satellite.

2. Theory

[6] In this section we present the theory developed for the accurate consideration of metal losses at waveguide junctions. After a brief review of the integral equation technique leading to the admittance matrix representation, we derive the novel expressions for the impedance matrix case. Next, the efficient implementation of both techniques is fully described.

[7] Let us consider a general lossy junction between two waveguides of arbitrary cross section as shown in Figure 1. According to Figure 1, the cross sections of the
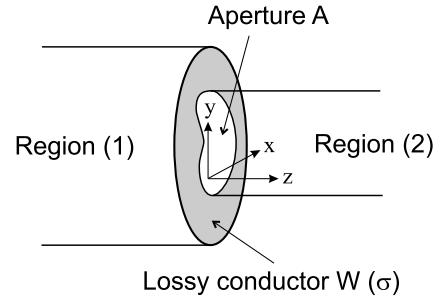

Figure 1. Lossy junction in the plane of the aperture ($z = 0$).

waveguides on each region ($\delta = 1, 2$) are defined as $CS(1) = A \cup W$ and $CS(2) = A$. The tangential electric and magnetic fields at each waveguide region are

$$\mathbf{E}_t^{(\delta)} = \sum_{n=1}^{\infty} V_n^{(\delta)} \mathbf{e}_n^{(\delta)} \qquad \mathbf{H}_t^{(\delta)} = \sum_{n=1}^{\infty} I_n^{(\delta)} \mathbf{h}_n^{(\delta)} \qquad (1)$$

where V_n and I_n are the modal voltages and currents, respectively, whereas $\mathbf{e}_n$ and $\mathbf{h}_n$ are the waveguide modal vector functions [see *Marcuvitz*, 1986].

2.1. Admittance Integral Equation Formulation

[8] For a good conductor, the boundary conditions of the tangential electric field are

$$\mathbf{E}_t^{(1)}(\mathbf{r}) = \mathbf{E}_t^{(2)}(\mathbf{r}) \quad \mathbf{r} \in A \qquad (2)$$

$$\mathbf{E}_t^{(1)}(\mathbf{r}) \approx Z_s \mathbf{J}_s(\mathbf{r}) \quad \mathbf{r} \in W \qquad (3)$$

where $\mathbf{J}_s(\mathbf{r})$ is the surface current density and Z_s is the surface impedance, which for good conductors can be approximated as follows [see *Balanis*, 1989]

$$Z_s = (1+j)R_s = (1+j)\sqrt{\frac{\omega\mu}{2\sigma}} \qquad (4)$$

As it is well known, in (4) ω represents the angular frequency, μ the magnetic permeability of the medium, and σ the metal conductivity.

[9] The original boundary conditions (2) and (3) can be rewritten as a single equation

$$\mathbf{E}_t^{(1)}(\mathbf{r}) - [1 - \xi(\mathbf{r})]Z_s\mathbf{J}_s(\mathbf{r}) = \xi(\mathbf{r})\mathbf{E}_t^{(2)}(\mathbf{r}) \quad \forall \mathbf{r} \in A \cup W$$
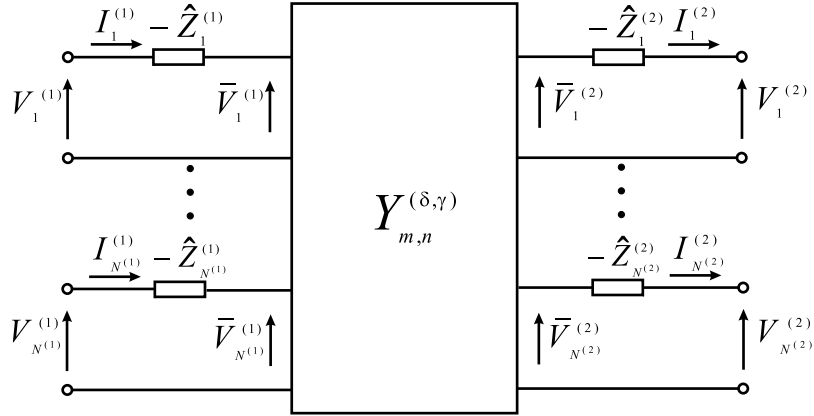
$$(5)$$

Figure 2. Generalized admittance matrix representation of the lossy waveguide junction.

where $\xi(\mathbf{r})$ is an auxiliary function defined in the following way

$$\xi(\mathbf{r}) = \begin{cases} 1 & \text{if } \mathbf{r} \in A \\ 0 & \text{elsewhere} \end{cases} \quad (6)$$

[10] Proceeding now as indicated by *Hueso et al.* [2004], we easily obtain the next two sets of Fredholm integral equations of the second kind

$$\mathbf{e}_n^{(1)}(s) = [1 - \xi(s)]Z_s\mathbf{N}_n^{(1)}(s)$$
$$+ \int\int_{CS(1)} \mathbf{N}_n^{(1)}(s')K^{(1)}(s,s')\,ds'$$
$$+ \xi(s)\iint_{CS(2)} \mathbf{N}_n^{(1)}(s')K^{(2)}(s,s')\,ds' \quad (7)$$

$$\xi(s)\mathbf{e}_n^{(2)}(s) = [1 - \xi(s)]Z_s\mathbf{N}_n^{(2)}(s)$$
$$+ \int\int_{CS(1)} \mathbf{N}_n^{(2)}(s')K^{(1)}(s,s')\,ds'$$
$$+ \xi(s)\int\int_{CS(2)} \mathbf{N}_n^{(2)}(s')K^{(2)}(s,s')\,ds' \quad (8)$$

where $\mathbf{N}_n^{(\delta)}$ are the unknown basis functions to be solved, whereas $K^{(1)}(s,s')$ and $K^{(2)}(s,s')$ are the kernels defined as

$$K^{(1)}(s,s') = \sum_{m=1}^{N^{(1)}} \hat{Z}_m^{(1)}\mathbf{e}_m^{(1)}(s) \cdot \mathbf{e}_m^{(1)}(s')$$
$$+ \sum_{m=N^{(1)}+1}^{\infty} Z_m^{(1)}\mathbf{e}_m^{(1)}(s) \cdot \mathbf{e}_m^{(1)}(s') \quad (9)$$

$$K^{(2)}(s,s') = \sum_{m=1}^{N^{(2)}} \hat{Z}_m^{(2)}\mathbf{e}_m^{(2)}(s) \cdot \mathbf{e}_m^{(2)}(s')$$
$$+ \sum_{m=N^{(2)}+1}^{\infty} Z_m^{(2)}\mathbf{e}_m^{(2)}(s) \cdot \mathbf{e}_m^{(2)}(s') \quad (10)$$

[11] In (9) and (10), $N^{(\delta)}$ means the number of accessible modes considered in each waveguide, whose concept was already introduced by *Rozzi and Meelenbrauker* [1975]. On the other hand, $Z_n^{(\delta)}$ is the modal impedance [see *Marcuvitz*, 1986], and $\hat{Z}_n^{(\delta)}$ denotes its asymptotic behavior as defined by *Hueso et al.* [2004]. For the accelerated evaluation of both kernels, it is recommended to follow the technique described in Appendix A.

[12] Once the two integral equations are solved as detailed in section 2.3, we can easily compute the admittance matrix elements of the lossy junction as follows

$$I_m^{(\delta)} = \sum_{n=1}^{N^{(1)}} \bar{V}_n^{(1)} Y_{m,n}^{(\delta,1)} - \sum_{n=1}^{N^{(2)}} \bar{V}_n^{(2)} Y_{m,n}^{(\delta,2)} \quad (11)$$

where

$$Y_{m,n}^{(\delta,\gamma)} = \iint_{CS(\delta)} \mathbf{N}_n^{(\gamma)}(s') \cdot \mathbf{e}_m^{(\delta)}(s')\,ds' \quad (12)$$

and the auxiliary voltages $\bar{V}_n$ are defined in Figure 2.

2.2. Impedance Integral Equation Formulation

[13] A completely dual procedure to the one just described before can be followed to formulate a generalized impedance matrix representation of the lossy waveguide junction. In this case, the starting equations are obtained from forcing the boundary
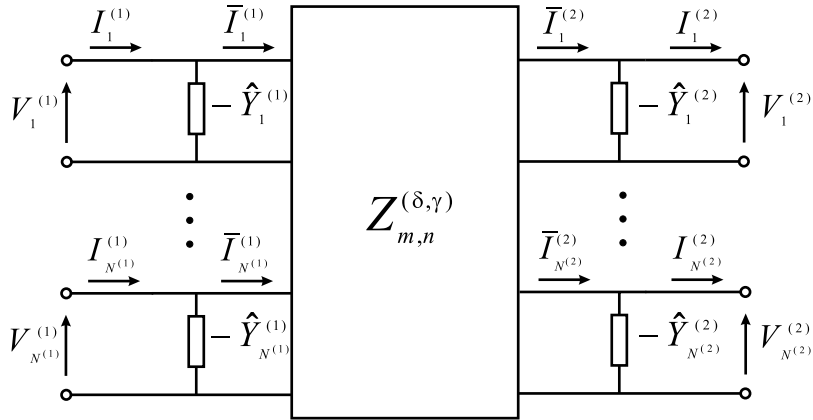
Figure 3. Generalized impedance matrix representation of the lossy junction.

conditions for the tangential magnetic field of a good conductor

$$\mathbf{H}_t^{(1)}(\mathbf{r}) = \mathbf{H}_t^{(2)}(\mathbf{r}) \quad \mathbf{r} \in A \tag{13}$$

$$Z_s \mathbf{H}_t^{(1)}(\mathbf{r}) \approx \hat{\mathbf{z}} \times \mathbf{E}_t^{(1)}(\mathbf{r}) \quad \mathbf{r} \in W \tag{14}$$

where Z_s is the surface impedance previously defined in (4), and equation (14) has been obtained taking vectorial products in both sides of equation (3)

$$\hat{\mathbf{z}} \times \mathbf{E}_t^{(1)}(\mathbf{r}) = Z_s \hat{\mathbf{z}} \times \left(\mathbf{H}_t^{(1)}(\mathbf{r}) \times \hat{\mathbf{z}} \right) \tag{15}$$

[14] It must be noted that equations (14) and (3) are completely dual if (14) is rewritten in terms of the metal surface admittance Y_s. For very good conductors, which is the most typical situation, it is well known that such admittance tends to infinity, thus requiring more terms in the series appearing in (14) to satisfy the equation. Therefore it can be expected that the impedance formulation will behave rather worse than the admittance one in terms of convergence speed.

[15] Now we can rewrite (13) and (14) as a single equation

$$\zeta(\mathbf{r})\mathbf{H}_t^{(1)}(\mathbf{r}) - [1 - \xi(\mathbf{r})]\left(\hat{\mathbf{z}} \times \mathbf{E}_t^{(1)}(\mathbf{r}) \right)$$
$$= \xi(\mathbf{r})\mathbf{H}_t^{(2)}(\mathbf{r}) \quad \forall \mathbf{r} \in A \cup W \tag{16}$$

where the following auxiliary function has been introduced

$$\zeta(\mathbf{r}) = \xi(\mathbf{r}) + Z_s(1 - \xi(\mathbf{r})) \tag{17}$$

Then, following a dual procedure to the one detailed by *Hueso et al.* [2004], we finally obtain the next two sets of Fredholm integral equations of the second kind

$$\zeta(s)\mathbf{h}_n^{(1)}(s) = [1 - \xi(s)]\mathbf{M}_n^{(1)}(s)$$
$$+ \zeta(s) \int \int_{CS(1)} \mathbf{M}_n^{(1)}(s')K^{(1)}(s, s') \, ds'$$
$$+ \xi(s) \int \int_{CS(2)} \mathbf{M}_n^{(1)}(s')K^{(2)}(s, s') \, ds' \tag{18}$$

$$\xi(s)\mathbf{h}_n^{(2)}(s) = [1 - \xi(s)]\mathbf{M}_n^{(2)}(s)$$
$$+ \zeta(s) \int \int_{CS(1)} \mathbf{M}_n^{(2)}(s')K^{(1)}(s, s') \, ds'$$
$$+ \xi(s) \int \int_{CS(2)} \mathbf{M}_n^{(2)}(s')K^{(2)}(s, s') \, ds' \tag{19}$$

where $\mathbf{M}_n^{(\delta)}$ are now the unknown basis functions. In this case, the two integral equation kernels $K^{(1)}(s, s')$ and $K^{(2)}(s, s')$ have dual expressions to the ones shown in (9) and (10) for the admittance case and can be simply obtained by replacing in such two equations $\hat{Z}_m^{(\delta)}$, $Z_m^{(\delta)}$ and $\mathbf{e}_m^{(\delta)}$ by $\hat{Y}_m^{(\delta)}$, $Y_m^{(\delta)}$ and $\mathbf{h}_m^{(\delta)}$, respectively. Therefore the acceleration technique described in Appendix A for the efficient computation of both kernels can also be followed.

[16] Once the unknown $\mathbf{M}_n^{(\delta)}$ basis functions are solved as shown in section 2.3, the impedance matrix elements of the lossy junction can be easily computed as

$$Z_{m,n}^{(\delta,\gamma)} = \iint_{CS(\delta)} \mathbf{M}_n^{(\gamma)}(s') \cdot \mathbf{h}_m^{(\delta)}(s') \, ds' \tag{20}$$

In this case, the generalized impedance matrix representation of the lossy junction is shown in Figure 3, where
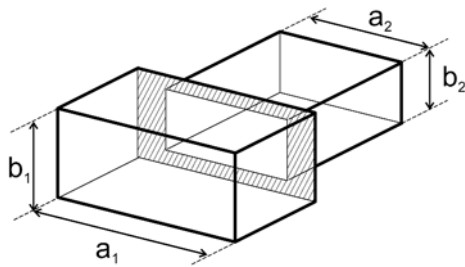
Figure 4. Centered waveguide step.

the presence of asymptotic modal admittances ($\hat{Y}_n^{(\delta)}$) in a shunt configuration can be seen.

2.3. Efficient Solution of the Integral Equations

[17] To solve the integral equations previously derived for the admittance and impedance matrix formulations, the well-known Galerkin version of the method of moments (MOM) described by *Harrington* [1992] will be employed. A different expansion for the basis functions, with respect to the one proposed by *Gerini et al.* [1998], has been used in this work. In our case, we have chosen modal solutions belonging only to region (1) (bigger waveguide), which has allowed us to achieve a complete set of modal

functions for expanding the unknown vector functions $\mathbf{N}_n^{(\delta)}$ ($\mathbf{M}_n^{(\delta)}$) for the admittance (impedance) formulation. Therefore

$$\mathbf{N}_n^{(\delta)}(s) \text{ or } \mathbf{M}_n^{(\delta)}(s) \approx \sum_{q=1}^{M^{(\delta)}} \alpha_q^{(n,\delta)} \mathbf{f}_q^{(1)}(s) \qquad (21)$$

$$s \in A + W, \ n = 1, 2, \ldots, N^{(\delta)}, \ \delta = 1, 2$$

where $\mathbf{f}_q^{(1)}$ will be $\mathbf{e}_q^{(1)}$ for the admittance case and $\mathbf{h}_q^{(1)}$ for the impedance formulation.

[18] Then the application of Galerkin's procedure provides a simple linear problem. The integral equations for both formulations can be handled in terms of a suitable defined linear operator $\mathcal{L}$ as shown next

$$\sum_{q=1}^{M^{(\delta)}} \alpha_q^{(n,\delta)} \langle \mathcal{L}\mathbf{f}_q^{(1)}, \mathbf{f}_p^{(1)} \rangle \approx \langle \mathbf{f}_n^{(\delta)}, \mathbf{f}_p^{(1)} \rangle \qquad (22)$$

where $p = 1, 2, \ldots, M^{(\delta)}$, thus obtaining $M^{(\delta)}$ equations with the same number of unknowns, and $\langle \cdot, \cdot \rangle$ means the usual inner product defined in the domain $A + W$.

[19] For the admittance formulation, the operator $\mathcal{L}$ acts in the following way

$$\mathcal{L}\mathbf{f} = [1 - \xi(s)] Z_s \mathbf{f}(s) + \int\int_{CS(1)} \mathbf{f}(s') K^{(1)}(s, s') \, ds'$$

$$+ \xi(s) \int\int_{CS(2)} \mathbf{f}(s') K^{(2)}(s, s') \, ds' \qquad (23)$$
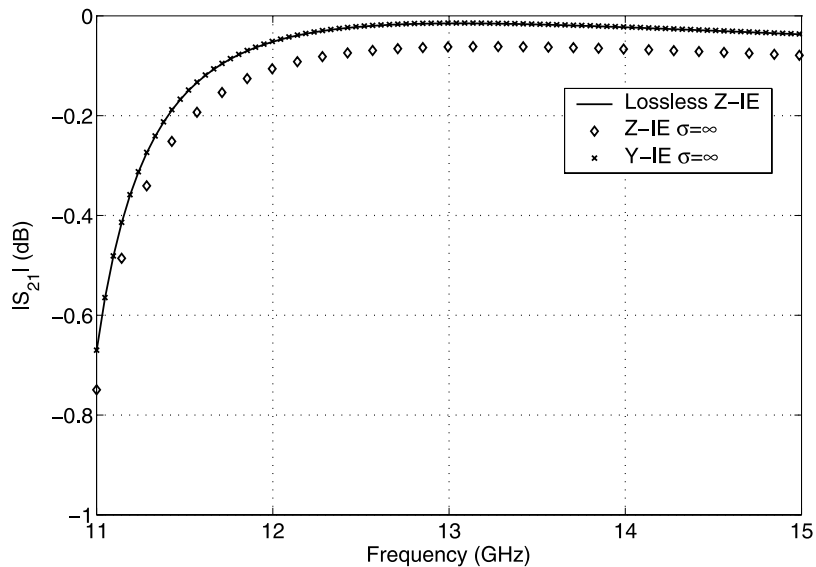

Figure 5. Magnitude of the transmission coefficient for a centered step considering a perfect conductor showing a comparison with the lossless Z-IE formulation. The input waveguide is a WR-75 (a_1 = 19.05 mm and b_1 = 9.525 mm), and the output waveguide dimensions are a_2 = 14 mm and b_2 = 7 mm.
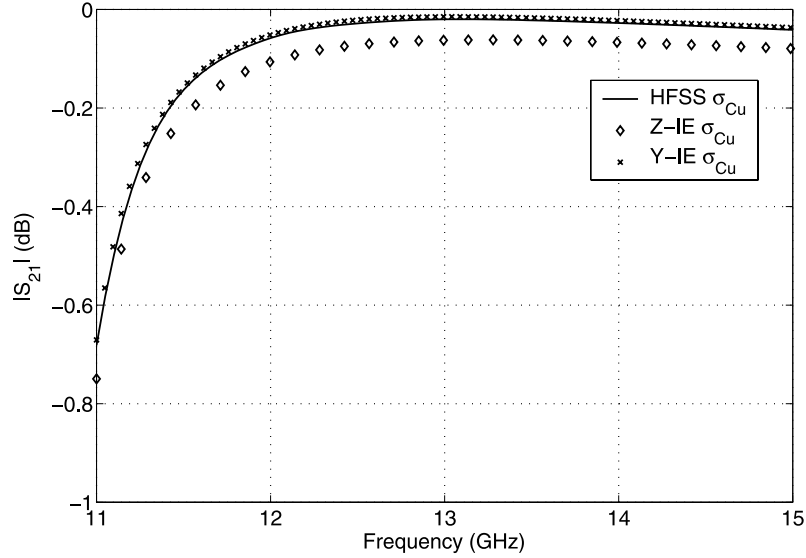
Figure 6. Magnitude of the transmission coefficient for a centered step made with copper ($\sigma_{Cu} = 5.8 \times 10^7$ S/m) showing a comparison with HFSS results. The dimensions are described in Figure 5.

whereas for the impedance case it is defined as follows

$$\mathcal{L}\mathbf{f} = [1 - \xi(s)]\,\mathbf{f}(s) + \zeta(s) \int\int_{CS(1)} \mathbf{f}(s')\,K^{(1)}(s, s')\,ds'$$
$$+ \xi(s) \int\int_{CS(2)} \mathbf{f}(s')\,K^{(2)}(s, s')\,ds' \qquad (24)$$

[20] From this point, the classical Galerkin approach can be easily followed. The operator $\mathcal{L}$ should be applied to each mode $\mathbf{e}_q^{(1)}$ (admittance case) or $\mathbf{h}_q^{(1)}$ (impedance case), and the expressions can be easily written in terms of coupling integrals among the modal vector functions of the waveguides involved in the lossy junction. For the efficient evaluation of such coupling integrals, the reader is referred to Appendix B.

3. Results

[21] To validate the theory presented in this paper, we have compared the loss effects predicted by our model with the numerical results provided by Ansoft HFSS v.8.5, as well as with experimental measurements. In this study, for comparative purposes, a Pentium IV platform running at 2.8 GHz with 1 GB DDRAM has been used for computing our results and those provided by HFSS.

[22] This section is organized as follows. First, a convergence study has been carried out in order to compare the admittance and impedance formulations. For that purpose, the losses introduced by the frontal walls of a simple waveguide step have been analyzed. Once the metal losses are accurately considered in the

waveguide junctions, the propagation losses in the waveguide sections connecting such junctions in real passive devices have been included following a classical perturbation approach. Then we have considered two real devices whose experimental electrical responses are available. The measured S parameters of an inductive filter for LMDS applications and of a satellite commercial filter are successfully compared with the simulated results provided by the proposed technique.

3.1. Convergence Study

[23] To start the validation of both formulations, we have chosen a simple waveguide step, shown in Figure 4,
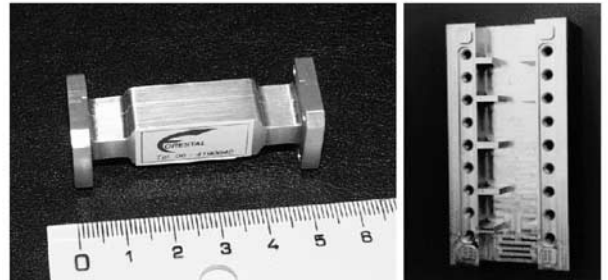

Figure 7. Photographs of a four-pole symmetric LMDS filter in WR-28 ($a = 7.112$ mm and $b = 3.556$ mm), where the inductive coupling irises have equal length (2.5 mm) and widths (4.939 mm, 3.799 mm, and 3.578 mm), and the cavities have equal width (8.636 mm) and lengths (4.696 mm and 5.555 mm).
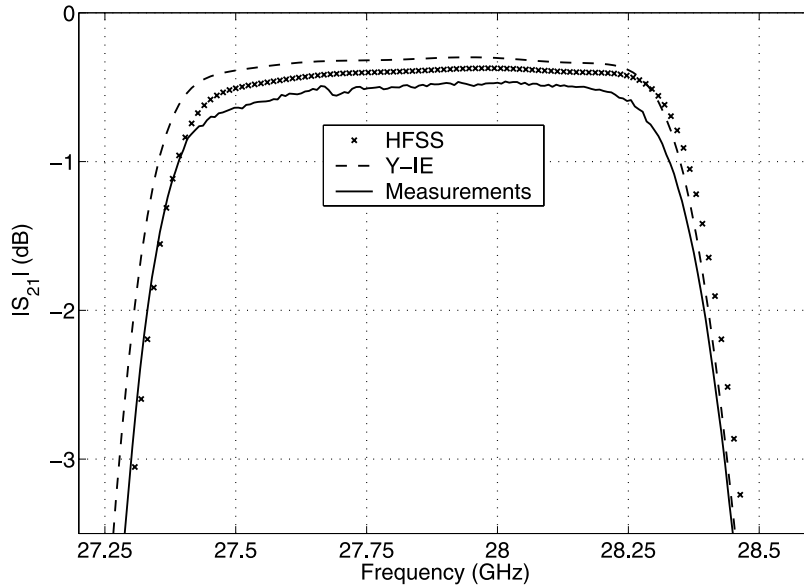
Figure 8. Detailed view of the insertion losses of the LMDS filter considering the conductivity value of the aluminum alloy. The Y-IE results are compared with HFSS data and experimental measurements.

where the shaded area has been first considered as a perfect conductor. For this limit case, the comparison is performed with the classical impedance integral equation (Z-IE) technique which does not consider losses in the device, already validated by *Gerini et al.* [1998] and therefore used as a reference.

[24] To get convergent results (see Figure 5), the reference method has required only one accessible mode, 70 basis functions for the Galerkin MOM, and 250 terms in the kernels. Both admittance and impedance matrix techniques results (considering a very high value for the metal conductivity) are also
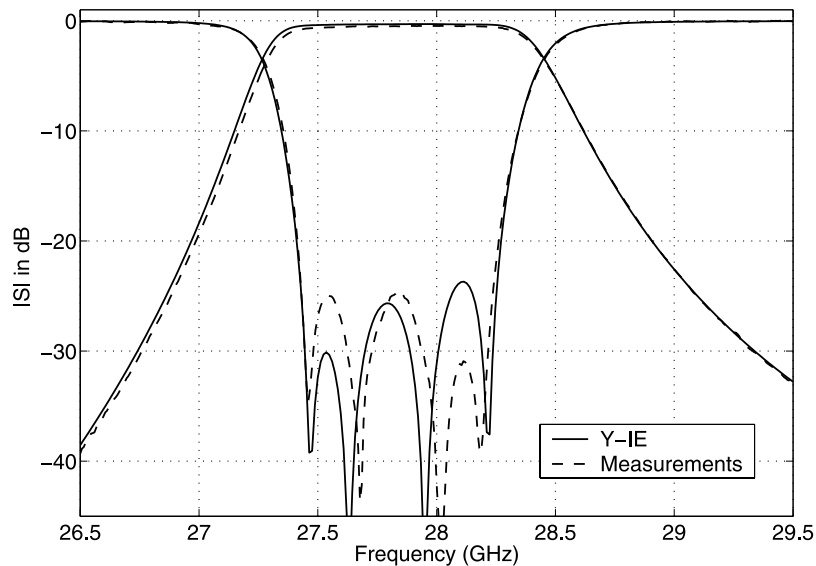

Figure 9. Magnitude of the *S* parameters of the LMDS filter considering the conductivity value of the aluminum alloy and comparing experimental measurements.

represented in Figure 5. We can see that the results provided by the admittance matrix formulation are very accurate, and they have been reached using only one accessible mode, 250 basis functions for the Galerkin MOM, and 400 terms in the kernels. On the other hand, in order to recover the less accurate results provided by the impedance matrix formulation (see Figure 5), one accessible mode, 2500 basis functions for the Galerkin MOM, and 8000 terms in the kernels have been required. Therefore the convergence is reached at a very high CPU cost in the case of the impedance formulation, as was already predicted theoretically in section 2.2. It is interesting to remark that this behavior is completely opposite to what happens in the lossless case, where impedance IE outperforms admittance IE, that is, in terms of convergence [see *Gerini et al.*, 1998].

[25] Once the two proposed formulations have been initially validated with a lossless case, we have studied the convergence behavior of both techniques for predicting the losses of the waveguide step shown in Figure 4 when the shaded area is made of copper ($\sigma_{Cu} = 5.8 \times 10^7$ S/m). In this case, the results provided by HFSS for such a lossy junction are selected as a reference.

[26] For comparative purposes, all the results for this lossy junction are shown together in Figure 6. As happened for the lossless case, the Y-IE formulation converges faster and better to accurate results than the Z-IE technique. In fact, to get the excellent results provided by the Y-IE algorithm, only 12 s were needed for solving 250 frequency points, whereas HFSS and Z-IE algorithm did require 60 and 1000 min, respectively. As a consequence, the admittance matrix formulation has been selected for the accurate analysis of real waveguide devices considered next.

3.2. LMDS Filter at 28 GHz

[27] Next, we have studied all loss effects in a four-pole filter used at the input front end of an LMDS receiver operating in the Ka band. A prototype of such filter has been made (see Figure 7) employing an aluminum alloy of conductivity equal to 1.2×10^7 S/m. This inductive and symmetric LMDS filter has been designed (see dimensions of the structure in the caption of Figure 7) to have a band-pass response of 800 MHz bandwidth centered at 28 GHz.

[28] In Figure 8, we can see a detailed view of the LMDS filter insertion losses. Figure 8 includes the simulated results using the Y-IE formulation and HFSS considering the conductivity value of the employed aluminum alloy, as well as a comparison with the experimental measurements of the prototype. As can be seen, our results agree with those given by the commercial software. However, the two simulated

FILTER1: 8-pole band pass filter				
Waveguide dimensions: WR-137 (34.85 × 15.85)				
Coupling window data				
Thick	2.0			
Width	$w1 = w9$	$w2 = w8$	$w3 = w7$	$w4 = w6$	$w5$
	22.050	16.300	14.490	14.100	14.000
Cavity data				
Length	$l1 = l8$	$l2 = l7$	$l3 = l6$	$l4 = l5$
	24.340	28.335	29.360	29.672
FILTER2: 6-pole low pass filter				
Waveguide width: 30.92				
Coupling window data				
Thick	4.0			
Height	$w1 = w7$	$w2 = w6$	$w3 = w5$	$w4$
	3.833	2.387	2.218	2.190
Cavity data				
Height	$h1 = h6$	$h2 = h5$	$h3 = h4$
	13.459	15.406	15.784
Length	$l1 = l6$	$l2 = l5$	$l3 = l4$
	7.8620	8.0940	8.1310
STEP TRANSFORMERS				
	Waveguide 1	Waveguide 2	Waveguide 3
Width	34.850	32.920	30.920
Height	15.850	10.600	7.1800
Length	10.000	17.614	10.000

Figure 10. Dimensions (in mm) of the C band filter.

results are slightly different from measurements, which can be attributed to several reasons. First, the real conductivity of a material can be altered from its nominal value by environment temperature and humidity. Besides, additional insertion losses can be introduced by each specific manufacturing technique. Finally, conductivity values are typically provided at zero frequency (direct current (DC)). However, at higher frequencies (microwaves and millimeter waves), such values can be affected by the surface properties, since the induced electrical current flows in smaller layers.

[29] To alleviate such small differences, or even for predicting conductivity values for unknown materials, we can make use of our accurate simulation tool in order to find an equivalent conductivity which allows us to recover experimental results. This process obviously needs previous measurements in order to calibrate the equivalent conductivity value. Proceeding in this way,
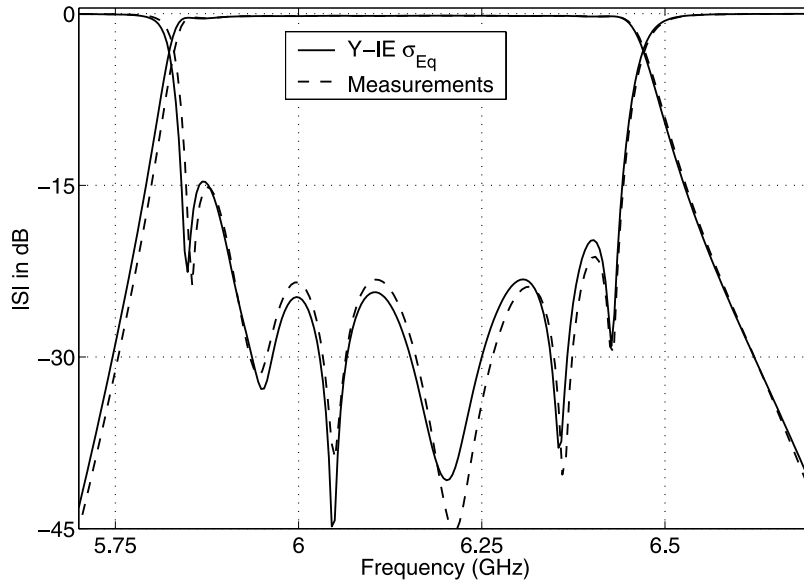
Figure 11. Magnitude of the S parameters for a commercial communications satellite filter considering the equivalent conductivity and comparing experimental measurements.

the loss effects in new manufactured filters using the same materials and fabrication techniques could be accurately predicted.

[30] The complete reflection and transmission responses of this LMDS filter are shown in Figure 9. To compute these results, our simulation tool only takes

14 min for 250 frequency points (3.4 s per frequency value), whereas HFSS requires about 140 min.

3.3. C Band Communication Satellite Filter

[31] Finally, a commercial communications satellite filter has been fully characterized. This device consists
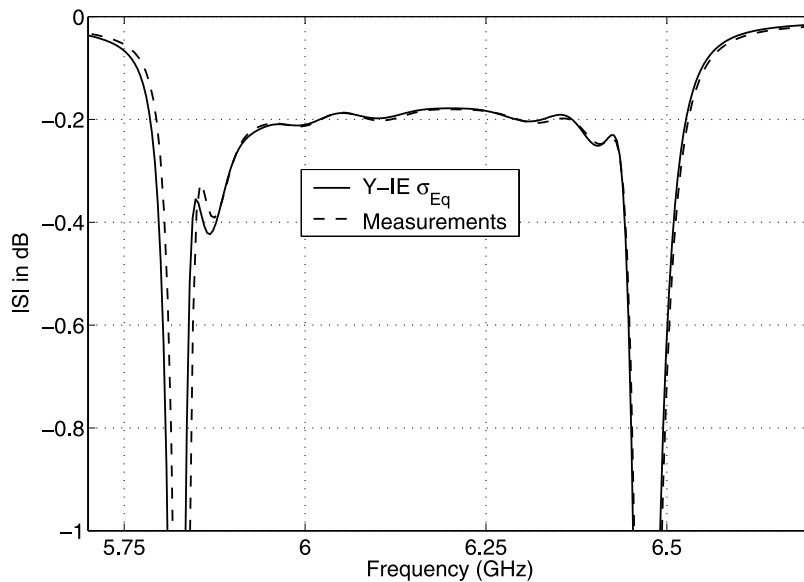

Figure 12. Detailed view of the magnitude of the S parameters for a commercial communications satellite filter considering the equivalent conductivity and comparing experimental measurements.

of the cascade of an eight-pole band-pass filter, a six-pole low-pass filter, and two double plane step transformers, and it has been designed for operating in the C band (see dimensions in Figure 10). A prototype was built using two aluminum blocks with subsequent silver plating and was measured experimentally by *Alvarez and Guglielmi* [1994].

[32] In this example, since we did not know a nominal value for the conductivity of the silver-plated aluminum, we found an equivalent conductivity value for such real material following the calibration procedure just described before ($\sigma_{Eq} = 3 \times 10^7$ S/m). As should be expected, this equivalent value is higher than the conductivity of the aluminum alloy used in the previous example (1.2×10^7 S/m) and smaller than pure silver (6.7×10^7 S/m). Using the predicted equivalent value, we computed the transmission and reflection parameters shown in Figure 11. A detailed view of the band-pass insertion losses is shown in Figure 12, which are approximately equal to 0.2 dB. The complete analysis of this device has only taken 52 min for 200 frequency points (i.e., 15.6 s per frequency value).

4. Conclusions

[33] Two extended integral equation techniques for the accurate consideration of losses in waveguide junctions are presented and evaluated. From this comparative study, we conclude that the impedance integral equation formulation does not offer good convergence results. On the contrary, the admittance formulation provides accurate loss characterization with very low CPU cost. The theory proposed for the lossy junctions has been combined with a classical perturbative approach for considering all loss effects present in passive waveguide structures. Successful results for two real filters used in LMDS and space applications have proved the accuracy and numerical efficiency of the proposed theory.

Appendix A: Efficient Computation of Integral Equation Kernels

[34] For this purpose, we have extended a procedure originally proposed by *Boria and Guglielmi* [1997] and already applied successfully to the lossless case by *Gerini et al.* [1998]. Proceeding in this way, the kernels of our two integral equation formulations can be evaluated as

$$K^{(\delta)}(s, s') = \hat{K}^{(\delta)}(s, s') - \sum_{r=1}^{R} k^{2r} \hat{\hat{K}}_{2r}^{(\delta)}(s, s') \qquad (A1)$$

where $\hat{K}^{(\delta)}$ and $\hat{\hat{K}}_{2r}^{(\delta)}$ have the following expressions

$$\hat{K}^{(\delta)}(s, s') = \sum_{m=1}^{\infty} \hat{X}_m^{(\delta)} \mathbf{f}_m^{(\delta)}(s) \cdot \mathbf{f}_m^{(\delta)}(s') \qquad (A2)$$

$$\hat{\hat{K}}_{2r}^{(\delta)}(s, s') = B_{2r} \sum_{m=N^{(\delta)}+1}^{\infty} \hat{X}_m^{(\delta)} \left(\frac{1}{k_{c,m}^{(\delta)}} \right)^{2r} \mathbf{f}_m^{(\delta)}(s) \cdot \mathbf{f}_m^{(\delta)}(s') \qquad (A3)$$

and R is usually set to 4, since it has been verified that it provides very accurate results in negligible computation time.

[35] In (A2) and (A3), $X_m^{(\delta)}$ and $\mathbf{f}_m^{(\delta)}$ mean $Z_m^{(\delta)}$ and $\mathbf{e}_m^{(\delta)}$ for the admittance case and $Y_m^{(\delta)}$ and $\mathbf{h}_m^{(\delta)}$ for the impedance formulation, respectively. In the admittance matrix formulation, we have for the TE case

$$B_{2r} = -\frac{1}{r! 2^r} \prod_{i=1}^{r} (2i - 1) = -\frac{1}{2}, -\frac{3}{8}, -\frac{5}{16}, -\frac{35}{128}, \cdots \qquad (A4)$$

and for the TM case

$$B_{2r} = -\frac{1}{r! 2^r} \prod_{i=1}^{r} (2i - 3) = \frac{1}{2}, \frac{1}{8}, \frac{1}{16}, \frac{5}{128}, \cdots \qquad (A5)$$

[36] For the impedance matrix formulation, because of duality, the expressions of the B_{2r} coefficients for the TE (TM) modes are the ones corresponding to the TM (TE) modes of the admittance case.

[37] Then, all of the infinite summations involved in the computation of the integral equation kernels are now frequency independent and can therefore be evaluated only once outside the frequency loop.

Appendix B: Efficient Evaluation of Coupling Integrals

[38] It should be pointed out that, in our case, the following new terms involving coupling integrals in the W region appear

$$A_{m,n} = \iint_W \mathbf{e}_m^{(1)}(s) \cdot \mathbf{e}_n^{(1)}(s) \, ds \qquad (B1)$$

[39] Obviously, the $A_{m,n}$ coupling integral would be $\delta_{m,n}$ if the integration domain was $A \cup W$, because of the well-known orthonormalization condition of standard modes [see *Marcuvitz*, 1986]. Using such normalization

property, these terms can be easily computed in the following way

$$
\begin{aligned}
A_{m,n} &= \int\!\!\int_W \mathbf{e}_m^{(1)}(s) \cdot \mathbf{e}_n^{(1)}(s)\,ds \\
&= \int\!\!\int_{A \cup W} \mathbf{e}_m^{(1)}(s) \cdot \mathbf{e}_n^{(1)}(s)\,ds - \int\!\!\int_A \mathbf{e}_m^{(1)}(s) \\
&\quad \cdot \mathbf{e}_n^{(1)}(s)\,ds \\
&= \delta_{m,n} - \int\!\!\int_A \mathbf{e}_m^{(1)}(s) \cdot \mathbf{e}_n^{(1)}(s)\,ds \qquad\text{(B2)}
\end{aligned}
$$

[40] In the previous expression, we have transformed an integration on the metallic wall W into an integration on the small aperture A (whose implementation is typically easier). In any case, the $A_{m,n}$ terms are frequency independent, and therefore they can also be computed outside the frequency loop. Following this procedure, the loss effects in passive waveguide components can be considered very efficiently.

References

Alvarez, A., and M. Guglielmi (1994), Multimode network representation of two dimensional steps in rectangular waveguides, paper presented at 24th European Microwave Conference, Cannes, France.

Alvarez, A., G. Connor, and M. Guglielmi (1996), New simple procedure for the computation of the multimode admittance or impedance matrix of planar waveguide junctions, *IEEE Trans. Microwave Theory Tech.*, *44*(3), 413–418.

Balanis, C. A. (1989), *Advanced Engineering Electromagnetics*, John Wiley, Hoboken, N. J.

Boria, V. E., and M. Guglielmi (1997), Accelerated computation of admittance parameters for planar waveguide junctions, *Int. J. Microwave Millimeter Wave Comput. Aided Eng.*, *7*(2), 195–205.

Collin, R. E. (1991), *Field Theory of Guided Waves*, Ser. Electromagn. Wave Theory, 2nd ed., IEEE Press, Piscataway, N. J.

Conciauro, G., M. Guglielmi, and M. Sorrentino (2000), *Advanced Modal Analysis: CAD Techniques for Waveguide Components and Filters*, John Wiley, Hoboken, N. J.

Gerini, G., M. Guglielmi, and G. Lastoria (1998), Efficient integral equation formulations for impedance or admittance representation of planar waveguide junction, in *1998 IEEE MTT-S International Microwave Symposium Digest*, edited by R. Meixner, E. Funk, and J. J. Cruz, pp. 1747–1750, IEEE Press, Piscataway, N. J.

Gustincic, J. (1963), A general power loss method for attenuation of cavities and waveguides, *IEEE Trans. Microwave Theory Tech.*, *1*(1), 83–87.

Harrington, R. F. (1992), *Field Computation by Moment Methods*, IEEE Press, Piscataway, N. J.

Hueso, J., S. Cogollos, B. Gimeno, V. E. Boria, A. Vidal, M. Taroncher, H. Esteban, and M. Guglielmi (2004), Accurate consideration of metal losses in planar waveguide junctions using an efficient integral equation technique, paper presented at MTT-S International Microwave Symposium, Inst. of Electr. and Electron. Eng., Fort Worth, Tex.

Itoh, T. (1989), *Numerical Techniques for Microwave and Millimeter-Wave Passive Structures*, John Wiley, Hoboken, N. J.

Leroy, M. (1983), On the convergence of numerical results in modal analysis, *IEEE Trans. Antennas Propag.*, *31*(7), 655–659.

Marcuvitz, N. (1986), *Waveguide Handbook*, IEE Electromagn. Waves Ser., vol. 21, Peter Peregrinus, London.

Mattes, M., and J. R. Mosig (1999), Calculation of ohmic losses in waveguide based components using an analytical technique, paper presented at 7th International Symposium on Recent Advances in Microwave Technology, Malaga, Spain.

Matthaei, G., L. Young, and E. M. T. Jones (1980), *Microwave Filters, Impedance-Matching Networks, and Coupling Structures*, Artech House, Norwood, Mass.

Melloni, A., and G. G. Gentilli (1995), Modellization of losses in TE011-mode waveguide bandpass filters, *IEEE Trans. Microwave Theory Tech.*, *43*(11), 2642–2644.

Rozzi, T. E., and W. F. G. Meelenbrauker (1975), Wide-band network modelling of interacting inductive irises and steps, *IEEE Trans. Microwave Theory Tech.*, *23*(2), 235–245.

Sorrentino, R., M. Mongiardo, F. Alessandri, and G. Schiavon (1991), An investigation of the numerical properties of the mode-matching technique, *Int. J. Numer. Modell.*, *4*, 19–43.

Trinchero, D., R. Tascone, P. Savi, and R. Orta (1997), Metal loss effect in the analysis of waveguide discontinuities, paper presented at ICEAA International Conference on Electromagnetic in Advanced Applications, Turin, Italy.

Wade, J. D., and R. H. McPhie (1990), Conservation of complex power technique for waveguide junctions with finite wall conductivity, *IEEE Trans. Microwave Theory Tech.*, *38*(4), 373–378.

———————

V. E. Boria, S. Cogollos, H. Esteban, J. Hueso, M. Taroncher, and A. Vidal, Departamento de Comunicaciones, Universidad Politécnica de Valencia, Casino de Vera s/n, E-46022 Valencia, Spain. (vboria@dcom.upv.es)

B. Gimeno, Instituto de Ciencia de los Materiales, Departamento de Física Aplicada, Universidad de Valencia, Dr. Moliner, 50, Burjasot, Valencia E-46100, Spain.

M. Guglielmi, European Space Research and Technology Centre, Kepleerlaan 1, Noordwijk N-2200AG, Netherlands.